

Supporting Information

Gold Labelling of Green Fluorescent Protein (GFP)-tag inside cells using recombinant nanobodies conjugated to 2.4 nm thiolate-coated gold nanoparticles

*Nadja Groysbeck, Mariel Donzeau, Audrey Stoessel, Anne-Marie Haeberle, Stéphane Ory, Danièle Spehner, Patrick Schultz, Ovidiu Ersen, Mounib Bahri, Dris Ihiawakrim, Guy Zuber**

Table of content

Materials and Methods (Addition to the main article)

Figure S1. DNA and amino acid sequences of GFP nanobody constructs and analysis of the construct stability as reported	S-7
Figure S2. Evaluation of the apparent binding affinities of GFP nanobody and mutated Nb-C7 for adsorbed GFP using ELISA.	S-8
Figure S3. Direct conjugation of nanobody to thiolate-coated AuNPs.	S-9
Figure S4. Analysis of Integrity of Nb- construct	S-10
Figure S5. Reaction products after addition of the thiolated E3 to AuG gold	S-11
Figure S6. Gold labeling of H2B-GFP HeLa using un-pepygylated Nb-AuNP conjugate.	S-12
Figure S7. Statistical analysis of (Nb-E3) ₂ :(K3) ₂ AuNP size distribution and clustering	S13
Figure S8. Fluorescent and (Nb-E3) ₂ :(K3) ₂ AuNP-mediated detection of protein-GFP fusions after transient gene transfection.	S14
Figure S9. Comparison of immunodetection ability of (Nb-E3) ₂ :(K3) ₂ AuNP into GFP-PCNA-interacting peptide (PIP) HeLa cells after fixation with 4%PFA or 2% PFA containing 0.02% glutaraldehyde	S15
Figure S10. Comparison of immunodetection ability of (Nb-E3) ₂ :(K3) ₂ AuNP in H2B-GFP HeLa cells fixed with 4% PFA or 2% PFA containing 0.02%glutaraldehyde.	S16
Figure S11. Preparation and analysis of the IgG-AuNP conjugate.	S17
Figure S12. Fluorescent and silver-enhanced images of H2B-GFP HeLa cells after IgG and IgG-AuNP -mediated detection of GFP.	S18

Figure S13. Fluorescent images of H2B-GFP HeLa cells after IgG-mediated detection of GFP. S19

Figure S14. Fluorescent images of H2B-GFP HeLa cells after IgG-mediated detection of GFP. S20

Figure S15. Analysis of (Nb-E3)₂:(K3)₂AuNP ability to detect GFP into H2B-GFP HeLa cells several days after assembly and evaluation of the sequential immunogold labelling methodology. S21

Figure S16. EDX spectroscopy analysis of a nuclear portion of H2B-GFP HeLa after gold immunolabeling with (Nb-E3)₂:(K3)₂AuNP without silver-enhancement. S22

Figure S17. EDX spectroscopy analysis of nuclear portion of the H2B-GFP HeLa specimen after gold immunolabeling with (Nb-E3)₂:(K3)₂AuNPs and silver enhancement. S23

Figure S18. Pre-embedding immuno-EM of the histone protein H2B-GFP with (Nb-E3)₂:(K3)₂AuNP. S24

Materials and Methods (Addition to the main article)

Materials: The AuG was synthesized as previously reported with a diameter of 2.4 nm.¹ The peptides were ordered from GeneCust in purity above 80%. The 2000 Da alpha-methoxy-omega-mercapto poly(ethylene glycol) (PEG) was ordered from Iris Biotech. Electron microscopy grade paraformaldehyde (20% w/v solution) and glutaraldehyde (25% w/v solution) were purchased from Electron Microscopy Sciences. Other reagents were obtained from Sigma Aldrich, Carl Roth, VWR Chemicals, Euromedex or Honeywell. They were used without further purification unless stated otherwise. All solutions and buffers were made with water purified with a Millipore Q-POD apparatus. Precision Plus Protein Standard Dual Xtra (BioRad) was used as protein ladder for SDS-PAGE analysis. The affinity-purified goat IgG directed against the nanobody domain was purchased from Jackson ImmunoResearch. The donkey anti-goat IgG (H+L) antibody conjugated to Alexa Fluor Plus 594 was purchased from Invitrogen. BSA-c was bought as 10% solution from Aurion. DNA transfection was performed with the *in vitro* transfection reagent jetOPTIMUS from Polyplus-transfection. Ni NTA agarose beads were purchased from Qiagen.

Specific equipment: A HI 2210 pH meter was used for measuring the pH of buffer solutions. Centrifugation of 50 mL tubes was done using an Eppendorf 5810R centrifuge equipped with an A-4-81 rotor. For smaller volumes (0.1 – 2 mL) centrifugation was performed in an Eppendorf 5415R centrifuge. AuNP reaction solutions were shaken on a Heidolph Rotamax 120 rocking platform. Functionalized AuNPs were concentrated and purified using Amicon Ultra 0.5 mL centrifugal devices (MWCO 30 kDa, if not stated otherwise).

Determination of AuNP concentration: Concentrations of AuNPs were determined spectrophotometrically by measuring the absorbance at 520 nm. The extinction coefficient of the AuNP was determined using the formula $\ln(\epsilon) = k \cdot \ln(D) + a$ reported by Liu *et al.*² ϵ = extinction coefficient ($M^{-1} \text{ cm}^{-1}$), D = AuNP core diameter in nm, $k= 3.32111$, $a = 10.80505$. From the measured diameter of 2.4 nm, the formula yields an $\epsilon_{520 \text{ nm}}$ of $89\,6771 \text{ M}^{-1} \text{ cm}^{-1}$ for AuG.

Denaturing and native polyacrylamide gel electrophoresis (PAGE) analyses: Denaturing sodium dodecylsulfate (SDS)-PAGE analysis was performed following a published protocol from Laemmli *et al.* on 15% or 5 – 18% polyacrylamide gradient gels. A 20 min pre-run at 20 mA was performed prior to loading the samples onto the gel. The AuNP samples were loaded onto the gel by dilution with 50% (v/v) glycerol to a final glycerol concentration of 5% (v/v). AuNPs were visible on the gels as black-brown bands. Proteins were revealed in blue by Coomassie blue staining. Titration of the non-covalent assemblies between (Nb-E3)₂ and (K3)₂AuNP before and after pegylation was performed by PAGE analysis in the absence of SDS.

Enzyme Linked Immunosorbent Assay (ELISA): The ELISA plates were prepared as follows: GFP (1 $\mu\text{g}/\text{mL}$ in PBS) was adsorbed onto wells of immunosorbent plates (Thermo Scientific) by an overnight incubation at 4°C. The remaining adsorbing surfaces were then blocked with 3% BSA in PBS (200 μL per well) for 1 h. Binding of AuNP-nanobody conjugates to plastic-adsorbed GFPs was then evaluated by incubating various concentrations of the conjugates (1 h, 100 μL per well). The bound conjugates were then detected with sequential incubation with a goat anti-V_HH Alpaca IgG (2.5 $\mu\text{g}/\text{mL}$, 1h), an anti-goat-HRP antibody (1:1000 dilution, 100 μL per well, 1 h) and then tetramethylbenzidine (TMB) (100 μL of a 10 mg/mL solution in 0.1 M sodium acetate, pH 6) in the presence of 0.007% hydrogen peroxide. Between incubations, the wells were washed three times with PBS containing 0.1% NP40 and three

times with PBS. Transformation of TMB in a colored product was stopped with 1 M sulfuric acid (50 μ L per well) and the color signal was measured with an ELISA plate reader (BioRad 550) at 450 nm. The binding of the AuNP-nanobody conjugates was alternatively evaluated by detection of the AuNP moiety. The binding of AuNP-nanobody conjugates to GFP-adsorbed surface was performed as described above. The AuNPs were then amplified in the dark for 15 min using a published silver developing solution.³

Cell Culture: Cells were cultured in a 37°C humidified incubator supplied with 5% CO₂. HeLa and stably transformed H2B-GFP HeLa cells were maintained in Dulbecco's modified Eagle medium containing 2 mM L-glutamine, 10 mM HEPES buffer, pH 7.0, 10% heat-inactivated fetal bovine serum (FBS) and 50 μ g/mL gentamycin. For immunocytochemistry, immunofluorescence and pre-embedding immuno-EM experiments, cells (25000 cells/well) were seeded into 24-well plates in 0.5 mL cell culture medium and were let to adhere on glass coverslips overnight.

Genetic engineering of the point mutation GFP nanobody variants : The GFP nanobody (Nb)⁴ was engineered to contain either a Serine 7 to Cysteine point mutation (C7-Nb), a Cterminal cysteine (C143-Nb) (Supporting information, Figure S1). Thiolated variants were constructed from the GFP nanobody gene using the PCR methodology and the following primers: 5'-GGAGAT ATACCA TGGGGT CCCAGG TTCAGC TGGTTG AATGTG GTGGTG-3' and 5'CACTAG TTGCGG CCGCTG AGGAGA CGGT-3'. The amplified DNA fragment was then digested with *NcoI* and *NotI* restriction enzymes and inserted into a pETOM vector encoding a c-myc sequence and a his6 tag.⁵

Expression and purification of anti-GFP nanobody variants: Recombinant his-tagged C7-Nb and C143-Nb were expressed in *E. coli* BL21(DE3)pLys after induction with 1 mM IPTG in 100 mL LB medium at 20°C for 24h. The bacteria were lysed by ultrasonication and the his-tagged proteins were purified by immobilized metal affinity chromatography using a HisTrap

HP column (1 mL) charged with NiSO₄ and then by gel filtration on a HiLoad Superdex 200 pg preparative column operating at a flow rate of 0.5 mL/min. Protein fractions were analyzed by SDS-PAGE. Selected fractions were pooled and protein solutions were concentrated with Amicon Ultra 4 mL centrifugal devices (MWCO 3 kDa).

Direct Au-S conjugation approach: A 40 μM solution of C7-Nb (75 μL, 3 nmol) was incubated with 0.4 mM TCEP (25 μL, 10 nmol) for 15 minutes at 25°C in 0.1 M HEPES, pH 7.5 to reduce disulfides to thiols. A portion of this mixture (88 μL of a 30 μM solution, 2.64 nmol) was then mixed with a 42 μM solution of the AuNP (250 μL, 10.5 nmol) to obtain a molecular AuNP/Nb ratio of 4. After an overnight incubation at 25°C, the alpha-methoxy-omega-mercapto poly(ethylene glycol) (818 μL of a 1 mM aqueous solution, 818 nmol) was added and the passivation reaction was allowed to proceed at 25°C for 2h. The released ligands and unreacted thiolated molecules were then separated from the AuNPs by ultrafiltration methodology using Amicon 30 K ultracentrifugal devices (5 washes with PBS). The fraction containing the AuNPs was further purified using Ni-NTA agarose beads (100 μL beads, equilibrated in PBS) by mixing the crude reaction mixture with the beads under mild agitation for 1.5 h in PBS. The beads were washed three times with PBS (1 mL), two times with 15 mM imidazole in PBS (1 mL) and the AuNP-nanobody conjugate was eluted with 500 μL of PBS containing 200 mM imidazole. The eluate was concentrated to a volume of 100 μL.

Transmission electron microscopy (Figure S6): Cellular specimens were imaged on a Hitachi H7500 transmission electron microscope (Hitachi High Technologies Corporation) equipped with an AMT Hamatsu digital camera (Hamatsu Photonics).

A. GFP Nanobody C7 mutant: DNA sequence

ATGCAGGTTCAACTGGTGGAAAGCGGCGGTGCTCTGGTACAACCGGGCGGTAGTCTGCGCCTG
 AGCTGTGCCGCAAGCGGTTTCCCAGTCAACCGCTACTCTATGCGTTGGTATCGCCAGGCGCCTG
 GTAAAGAACGTGAATGGGTTGCCGGCATGAGCAGTGC GGCGCATCGTTCTAGTTACGAGGACTC
 TGTTAAAGGTCGTTTTACAATTAGCCGTGATGATGCGCGCAATACCGTGTATCTGCAAATGAACA
 GTCTGAAGCCGGAGGACACCGCAGTATATTATTGCAATGTCAACGTGGGGTTTGAATATTGGGGC
 CAGGGGACTCAGGTGACGGTGAGCTCTAAACATCACCATCACCATCAC

Amino acid sequence of the GFP Nanobody Nb-C7

mQVQLVE^SCGGALVQPGGSLRLSCAASGFPVNRYSMRWYRQAPGKEREWVAGMSSAGDRSSYEDS
 VKGRFTISRDDARNTVYLQMNSLKPEDTAVYYCNVNVGFYWGQGTQVTVSSKHHHHHH

B. GFP Nanobody-C143: DNA sequence

ATGGGGTCCCAGGTTCACTGGTTGAAAGTGGTGGTGCCTGGTACAACCGGGCGGTAG
 TCTGCGCCTGAGCTGTGCCGCAAGCGGTTTCCCAGTCAACCGCTACTCTATGCGTTGGTA
 TCGCCAGGCGCCTGGTAAAGAACGTGAATGGGTTGCCGGCATGAGCAGTGC GGCGCATC
 GTTCTAGTTACGAGGACTCTGTTAAAGGTCGTTTTACAATTAGCCGTGATGATGCGCGCAAT
 ACCGTGTATCTGCAAATGAACAGTCTGAAGCCGGAGGACACCGCAGTATATTATTGCAATGT
 CAACGTGGGGTTTGAATATTGGGGCCAGGGGACCCAGGTCACCGTCTCCTCAGCGGCCG
 CAACTAGTGAACAAAACATCTCAGAAGAGGATCTGCGCGCTAGCGCACATCACCATCA
 TCACCATTGT

Amino acid sequence of the GFP Nanobody Nb-C143

mGSQVQLVESGGALVQPGGSLRLSCAASGFPVNRYSMRWYRQAPGKEREWVAGMSSAGDR
 SSYEDSVKGRFTISRDDARNTVYLQMNSLKPEDTAVYYCNVNVGFYWGQGTQVTVSSAAAT
 SEQKLISEEDLRASAHHHHHH**C143**

C. Analysis of the stability at 4°C of purified Nb-C7 and Nb-C143 21 days after purification showed fast degradation of the Nb-C143

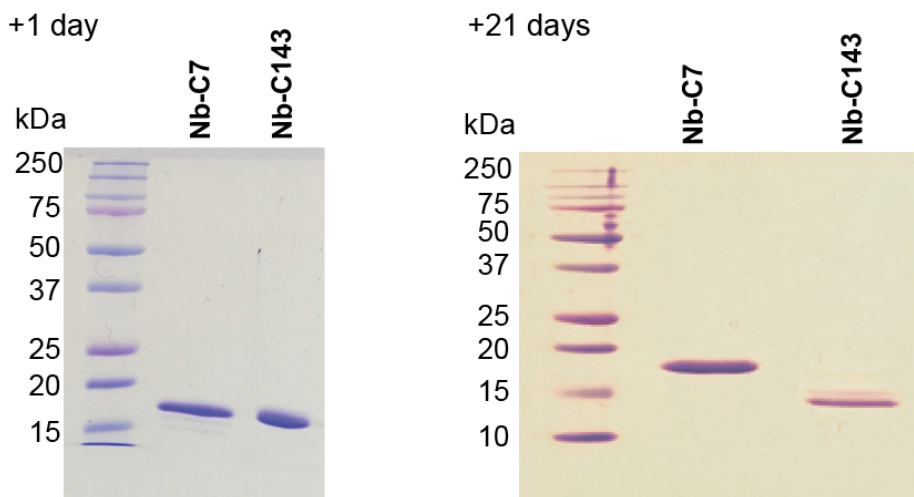


Figure S1. A and B. DNA and amino acid sequences of GFP nanobody constructs. C. Analysis of the construct stability as reported.

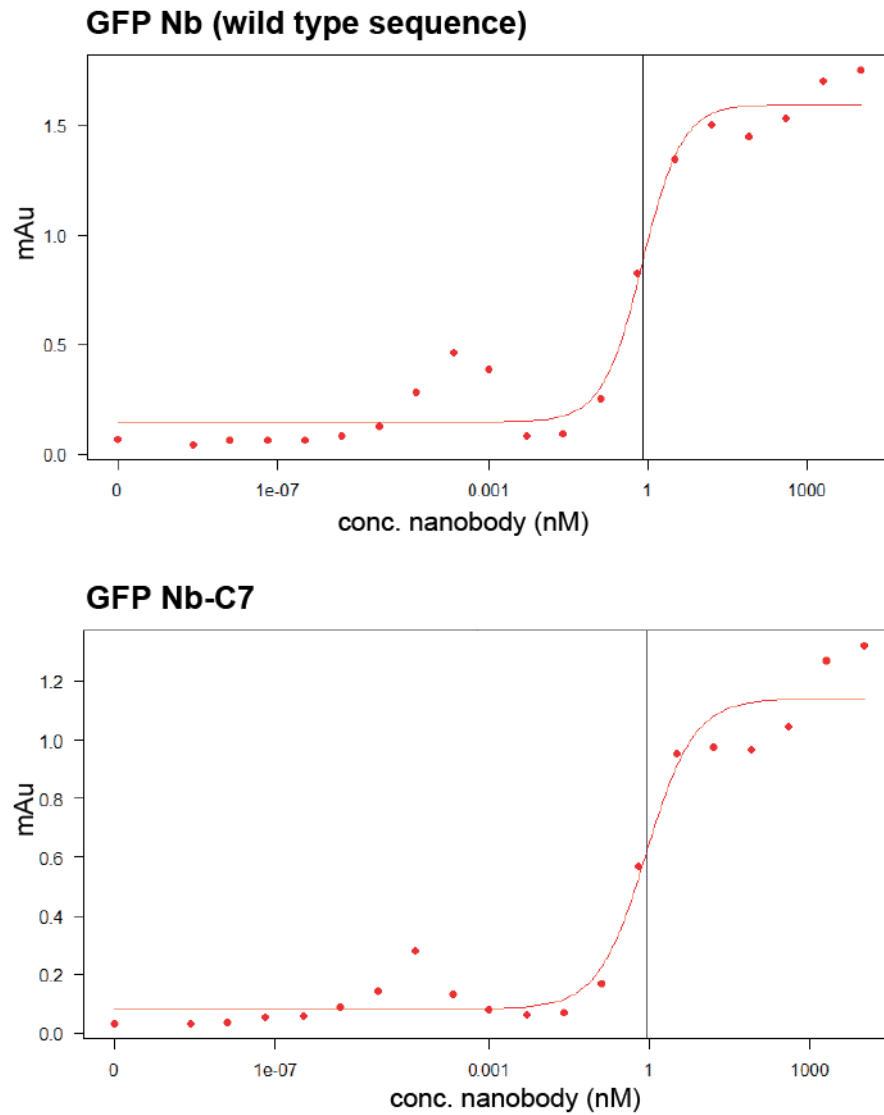


Figure S2. Evaluation of the apparent binding affinities of GFP nanobody and mutated Nb-C7 for adsorbed GFP using ELISA. Data revealed apparent K_{ds} of 0.78 and 0.87 nM for the wt Nb and Nb-C7 respectively, suggesting that the point mutation did not alter the apparent affinity of the nanobody for GFP.

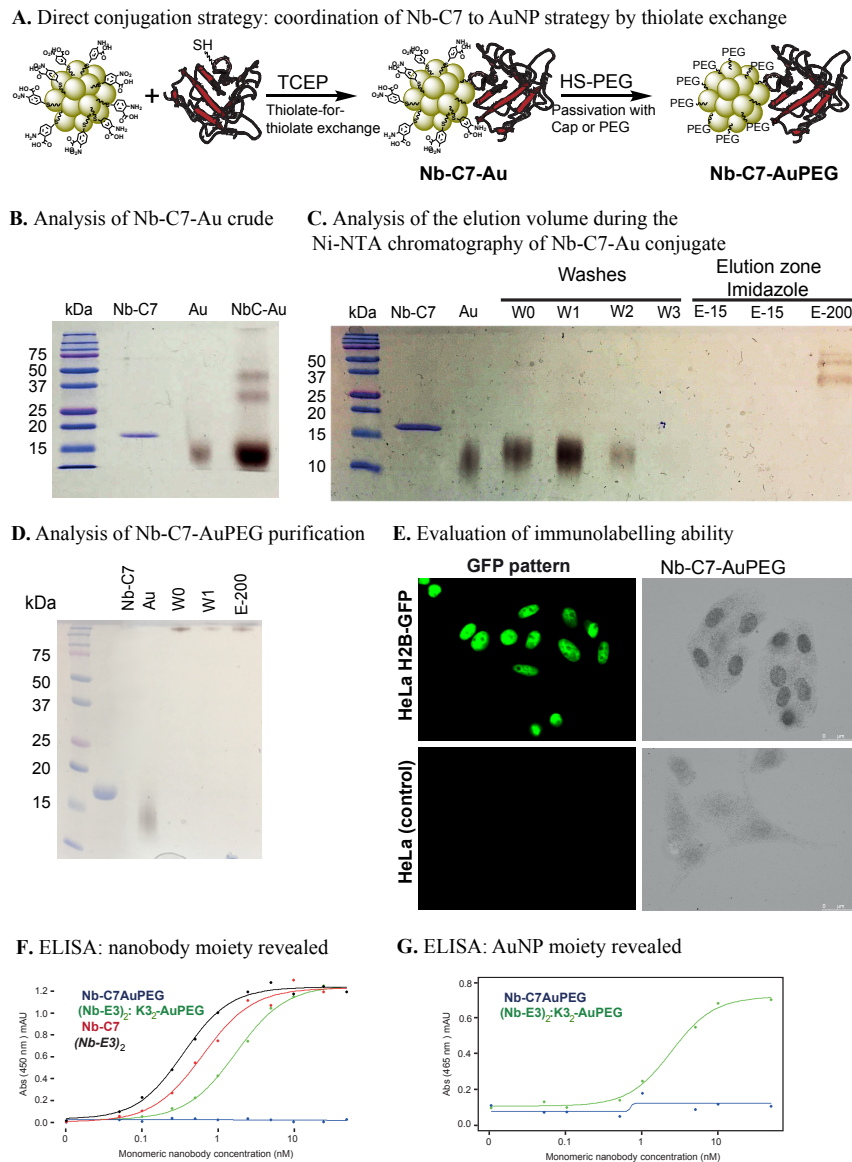


Figure S3. A. Illustration of the direct conjugation of nanobody to thiolate-coated AuNPs. The point mutated C7 nanobody (Nb-C7) was added to TNB/TAB-coated AuNP to obtain the Nb-C-Au by thiolate exchange. TNB/TAB ligands were further exchanged with thiolated PEG for passivation. B. SDS-PAGE of crude products (Nb-C-Au) of reaction between the AuNP (Au) and the thiolated nanobody (Nb-C7) as indicated. B. SDS-PAGE showing affinity purification of unpegylated Nb-C-Au using Ni NTA agarose beads. W0-W3 = wash fractions (PBS), E-15 mM: PBS fractions containing 15 mM imidazole. E-200: PBS with 200 mM imidazole, yielding NbCAu. D. Analysis of the eluted fractions from the Ni-NTA chromatography for purification of NbC-AuPEG. E. Fixed and permeabilized cells were incubated with NbC-AuPEG and then washed to remove unbound probes. The conjugates were revealed by silver staining. F and G. Evaluation of the binding ability of the probes for adsorbed GFP. The bound probes were detected using either anti-Nb antibody (F) or silver (G). Data demonstrate that the Nb-C-AuPEG does not bind to GFP.

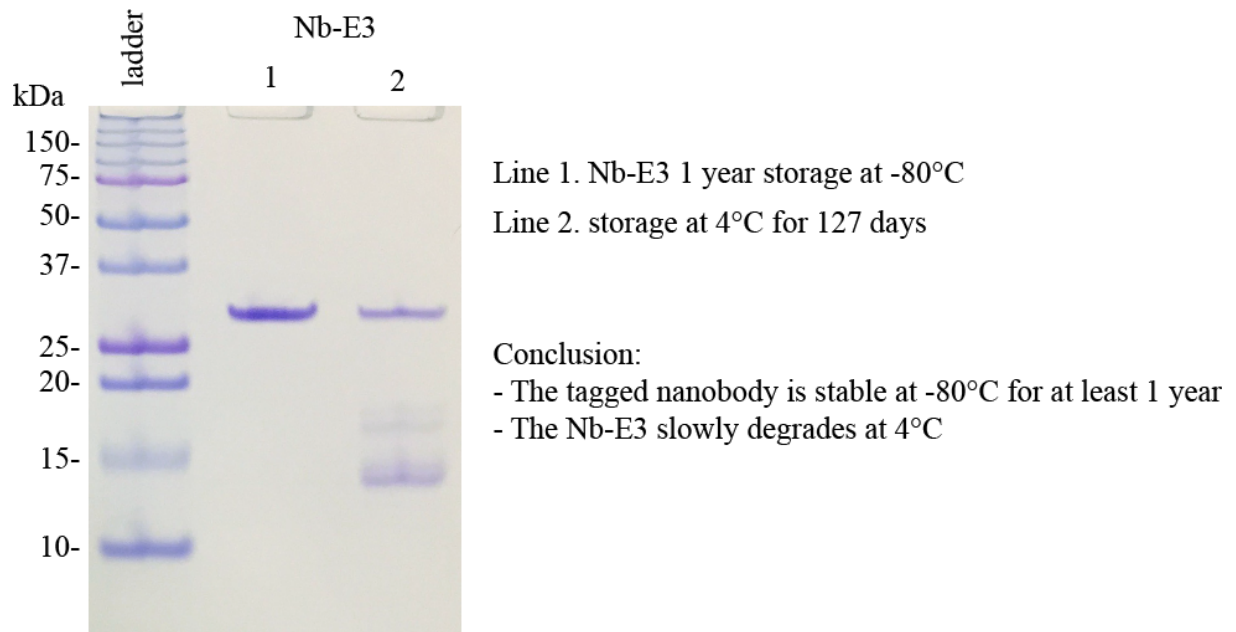


Figure S4. PAGE Analysis of the Nb-E3 construct integrity after storage at -80°C for > 1 year (line 1) and storage at 4°C for 127 days (line 2).

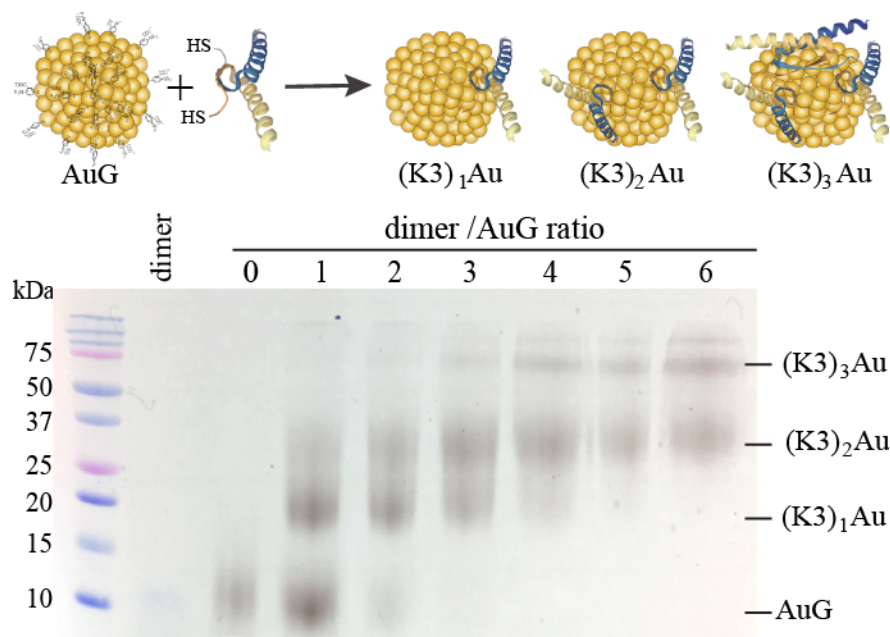
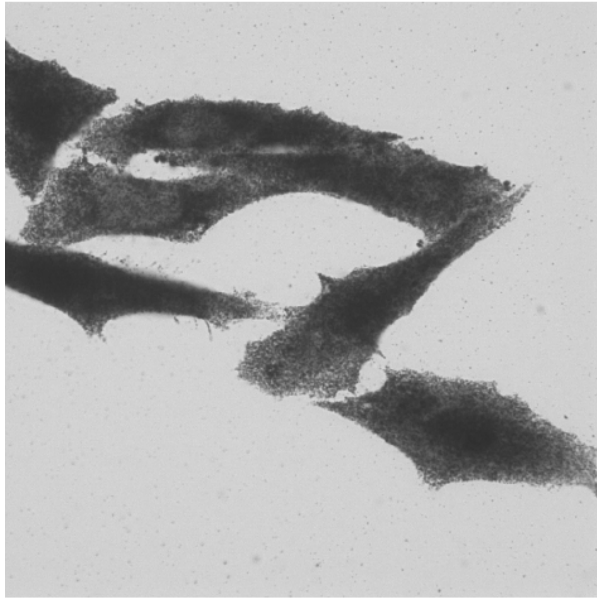


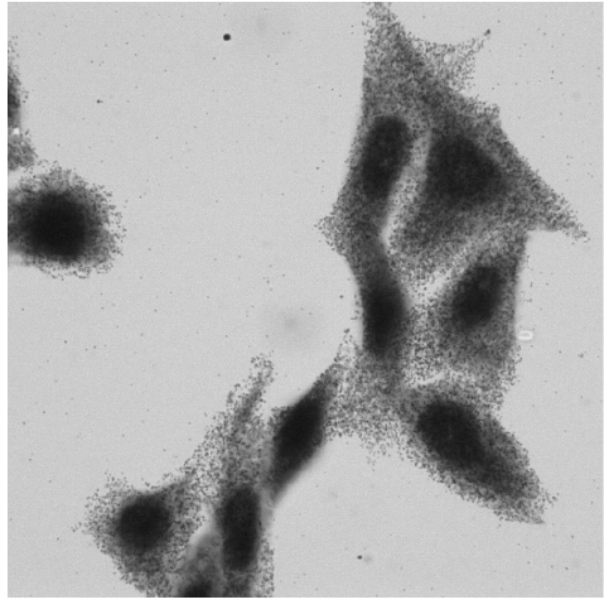
Figure S5. Synthetic scheme and PAGE analysis of the reaction products after addition of the thiolated peptide dimer to AuG gold nanoparticle in water at the indicated dimer/AuG molar ratio.

A. GFP labeling of fixed cells using $(\text{Nb-E3})_2:(\text{K3})_2\text{Au}$ (unpegylated)

HeLa wild type - control-

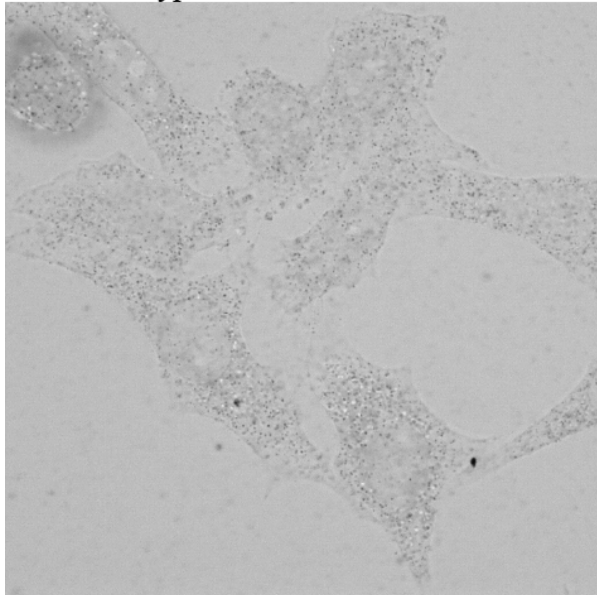


H2B-GFP HeLa



B. GFP labeling of fixed cells using pegylated $(\text{Nb-E3})_2:(\text{K3})_2\text{Au}$

HeLa wild type - control-



H2B-GFP HeLa

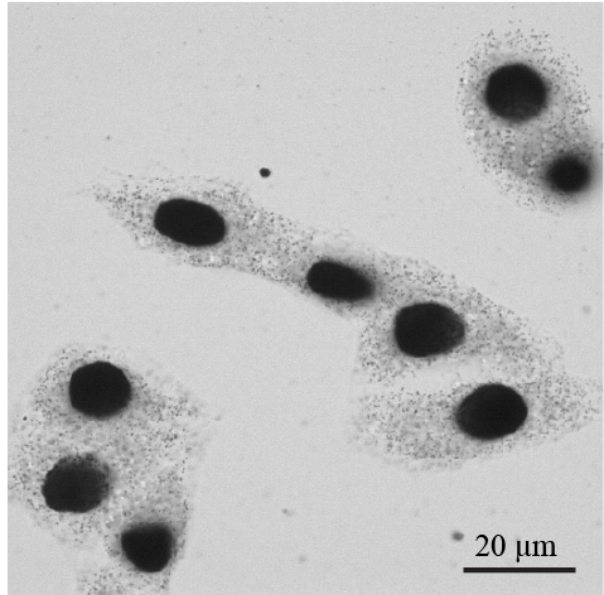
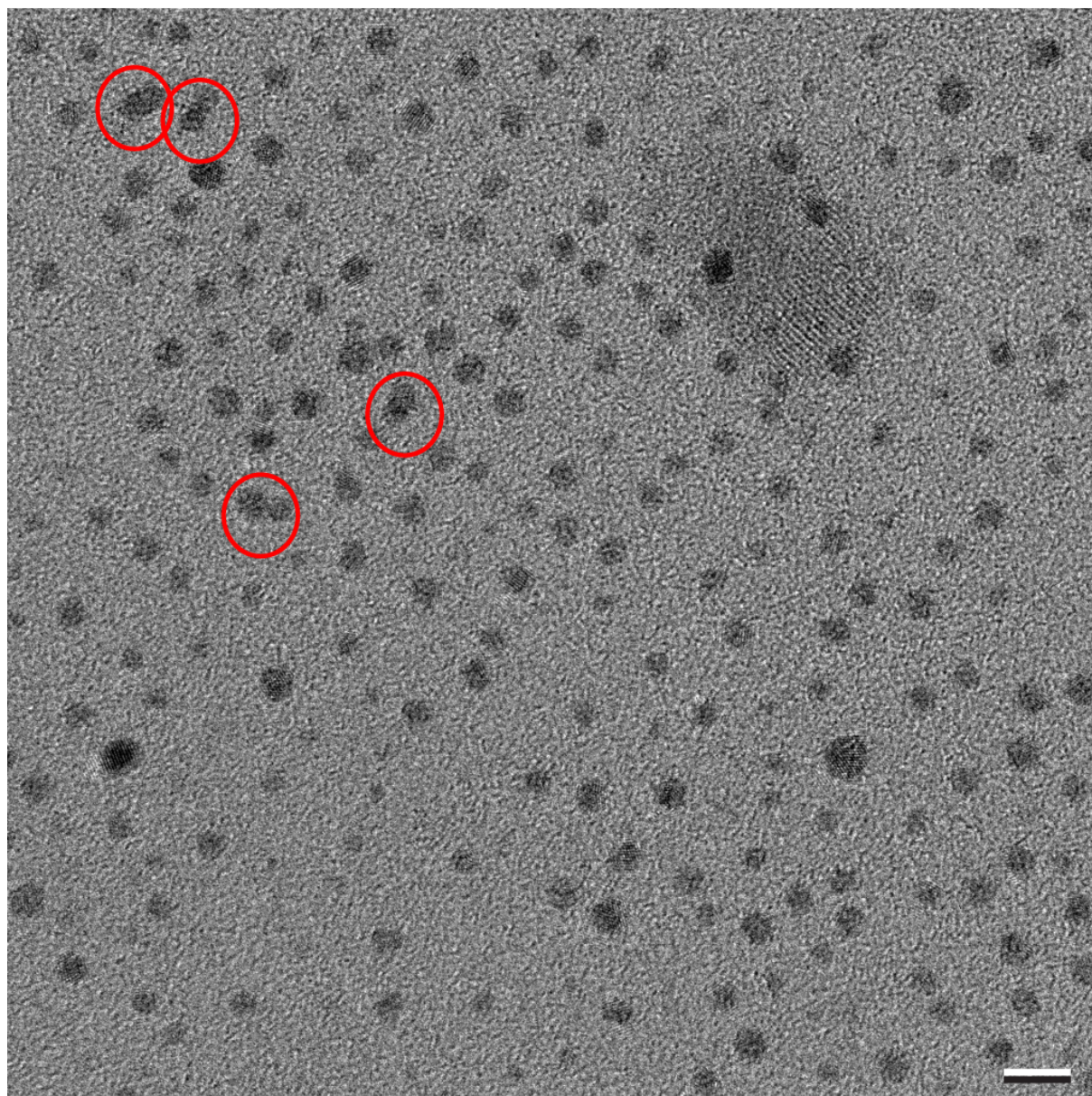


Figure S6. Light microscopy images of GFP labeling of fixed cells HeLa and H2B-GFP HeLa using unpegylated and the pegylated $(\text{Nb-E3})_2:(\text{K3})_2\text{AuNP}$ probes as indicated. The cell membrane was permeabilized. The cells were then incubated with 6 nM of the $(\text{Nb-E3})_2:(\text{K3})_2\text{AuNP}$ conjugates, washed, and the gold nanoparticles bound to cellular components were detected by extensive silver enhancement.

TEM image of $(\text{Nb-E3})_2:(\text{K3})_2$ AuNP



5 nm

Statistical analysis:

Number of counted particles: 180

Mean diameter: 2.31 nm

Mediane diameter: 2.38 nm

Standard deviation: 0.35 nm

Dual particles: 4 (2.2%) as indicated by circle

Figure S7. Image used for measuring the size of the gold nanoparticle of $(\text{Nb-E3})_2:(\text{K3})_2$ AuNPs and the eventual clustering. Out of the 180 particles present in the field, 4 couples as marked by the red circle were observed.

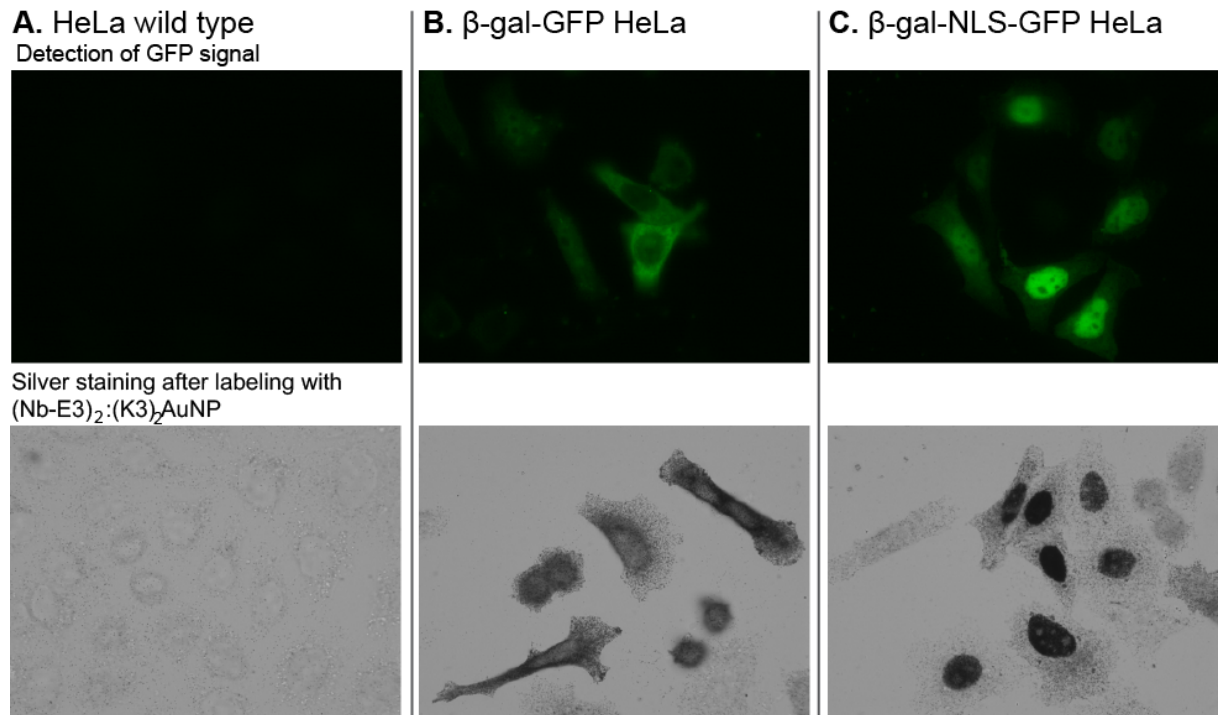
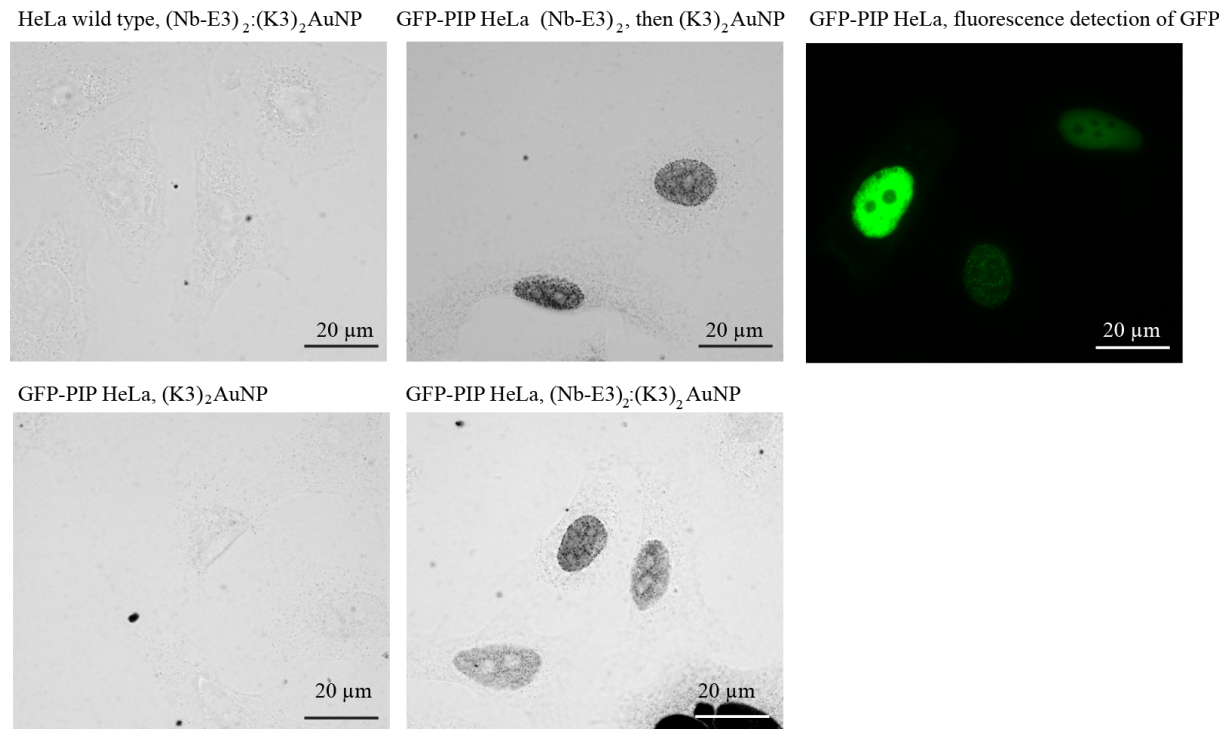


Figure S8. Fluorescent and $(\text{Nb-E3})_2:(\text{K3})_2\text{AuNP}$ -mediated detection of protein-GFP fusions after transient gene transfection. HeLa cells were transiently transfected with DNA plasmids to express β -Galactosidase-GFP (β -Gal-GFP) or β -Galactosidase-Nuclear Localization Signal-GFP (β -Gal-NLS-GFP). Upper images: Detection of the GFP signal in PFA-fixed HeLa cells 24 after DNA plasmid transfection. Lower images: The cell membrane was further permeabilized. The cells were incubated with 6 nM $(\text{Nb-E3})_2:(\text{K3})_2\text{AuNP}$, washed and the gold nanoparticles bound to cellular components were detected by extensive silver enhancement.

A. Fixation: 4% PFA, Permeabilization: 0.1% Triton X-100



B. Fixation: 2% PFA, 0.02% Glutaraldehyde, Permeabilization: 0.1% Triton X-100

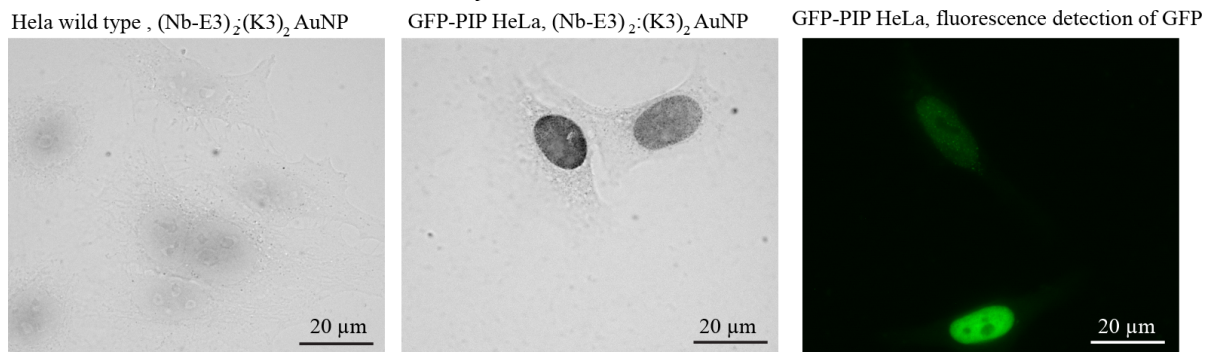
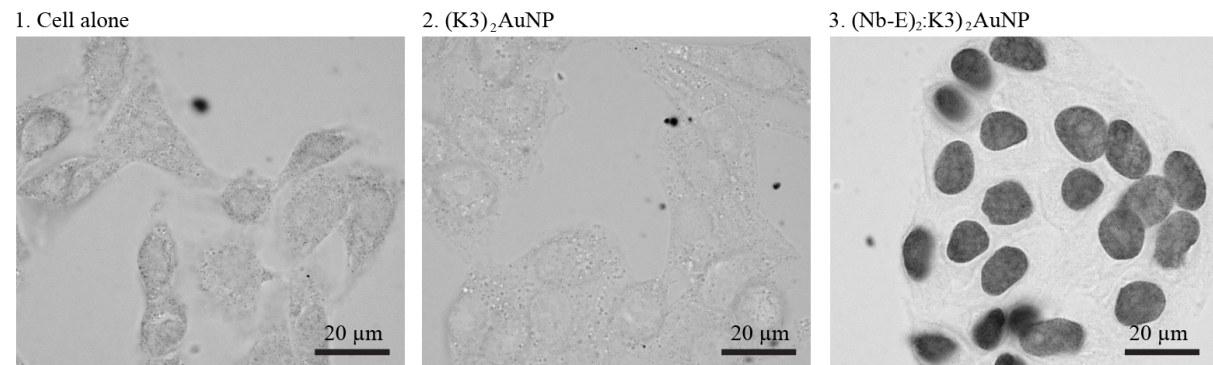


Figure S9. Comparison of immunodetection ability of (Nb-E3)₂:(K3)₂AuNP into GFP-PCNA-interacting peptide (PIP) HeLa cells after fixation with 4%PFA or 2% PFA containing 0.02% glutaraldehyde.⁶ The GFP-PIP expressing HeLa cells were obtained by transfection of HeLa cells with a modified PEI⁷ and the plasmid fusion (pβA-eGFP-con1-NLS) encoding the GFP-PIP under the control of the β-actin promoter.⁵ 24h after transfection, the cells were fixed for 30 min in 0.2M HEPES, PH 7.4, containing either 4% PFA or 2% PFA, 0.02% glutaraldehyde. The cells were then permeabilized with 0.1% Triton X-100 in PBS. The HeLa cells were then incubated with: - (K3)₂AuNP, ; - (Nb-E3)₂, 3 washing steps (3 times 0.3% BSAC in PBS) and (K3)₂AuNP; - (Nb-E3)₂:(K3)₂AuNP (16 nM). Solution of incubation was PBS containing 10% FBS. After the washing steps, the specimen-bound gold particles cells were detected after silver enhancement. Fluorescent images showed that 80% of the cells were expressing nuclear PIP-GFP at various levels.

A. Fixation: 4% PFA, Permeabilization: 0.1% Triton X-100



B. Fixation: 2% PFA, 0.02% Glutaraldehyde, Permeabilization: 0.1% Triton X-100

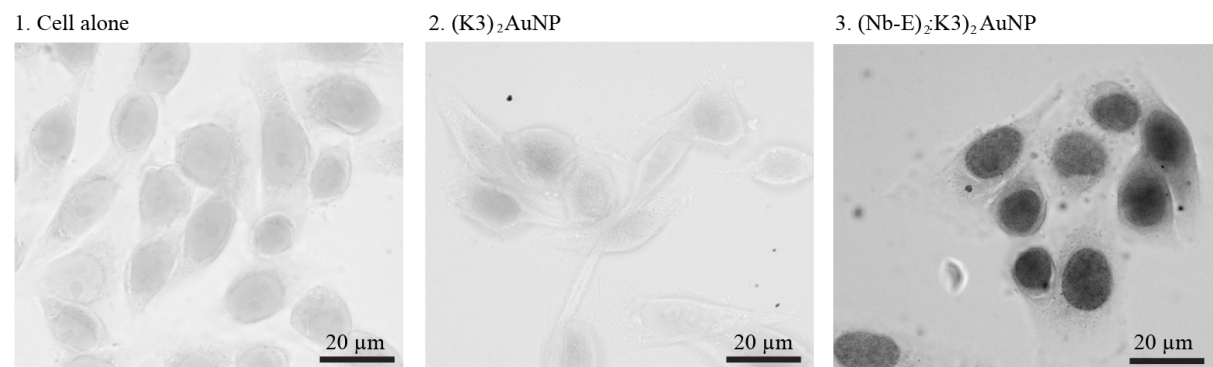
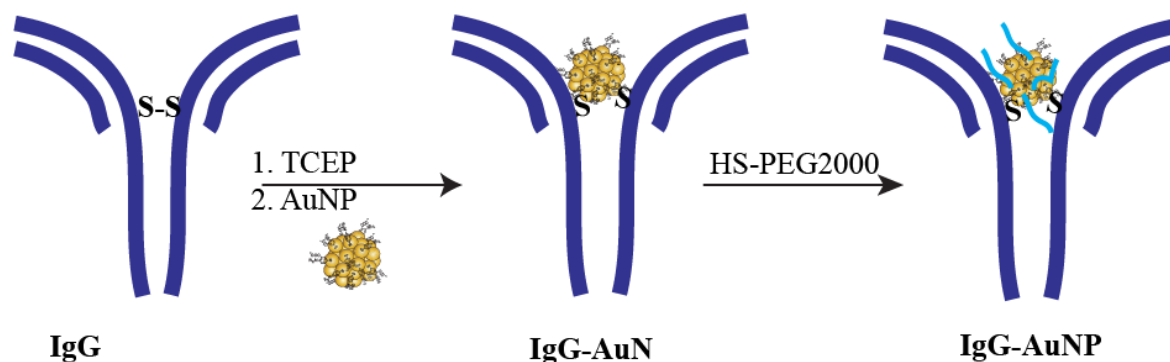


Figure S10. Comparison of immunodetection ability of $(Nb-E3)_2:(K3)_2AuNP$ in H2B-GFP HeLa cells fixed with 4% PFA or 2% PFA containing 0.02% glutaraldehyde.⁶ The H2B-GFP cells were fixed for 30 min in 0.2M HEPES, PH 7.4, containing either 4% PFA or 2% PFA, 0.02% glutaraldehyde. After fixation, the cells were permeabilized with 0.1% Triton X-100 in PBS (20min). The H2B-GFP HeLa cells were then incubated with $(K3)_2AuNP$ and $(Nb-E3)_2:(K3)_2AuNP$ (16 nM) in PBS containing 10% FBS. After the washing steps, the specimen-bound gold particles cells were detected by silver enhancement.

A. Scheme for conjugation and passivation of AuNP to a mouse anti-GFP IgG



B. PAGE analysis

1. Coomassie blue staining

2. Coomassie blue then silver staining

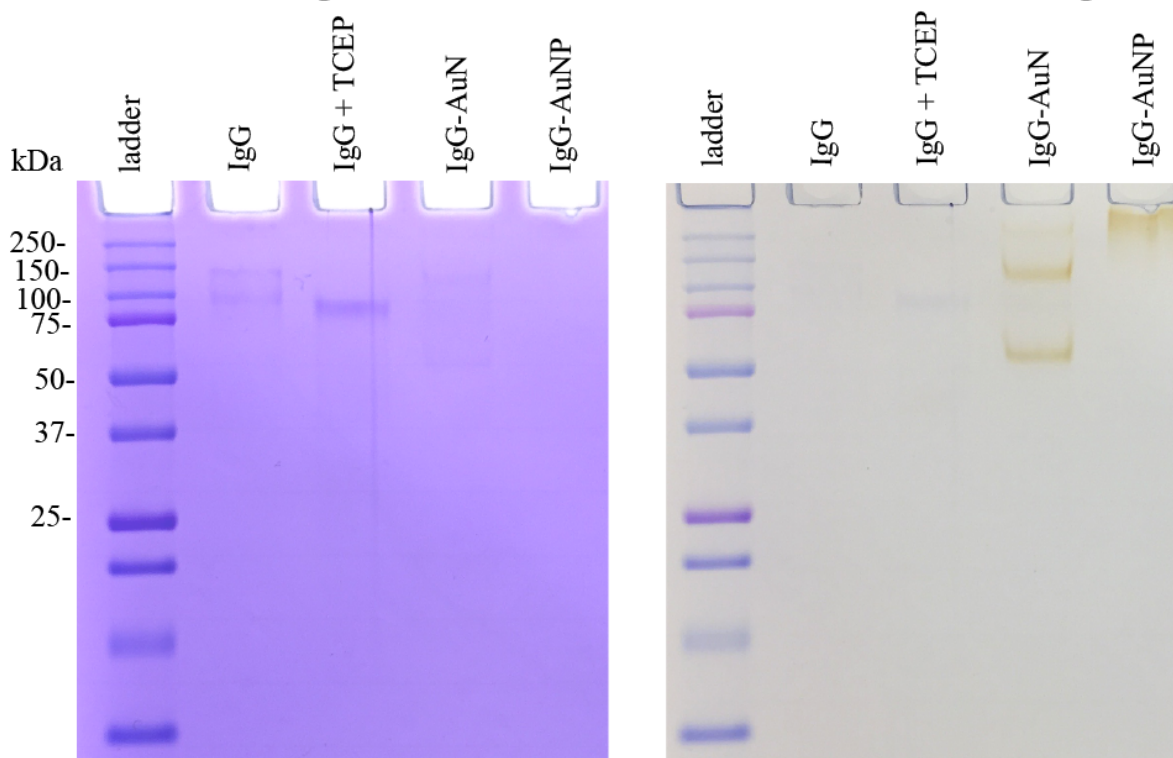
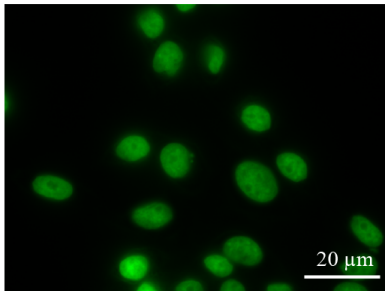


Figure S11. Preparation and analysis of the IgG-AuNP conjugate. A. Schematic route to the preparation of the anti-GFP-gold nanoparticle conjugate. The mouse antibody (clone GFP-2A3, IGBMC, Strasbourg) was incubated with 1 mM TCEP for 6 h. The raw mixture was then reacted for 12 hours with the TAB-, TNB- coated AuNP (1.5 equivalent). The conjugate was then purified by size exclusion (BioRad P100, elution PBS). The conjugate (IgG-AuN) was then reacted with thiolated PEG2000 (40 equivalents) for passivation of the remaining exchangeable TAB and TNB ligands onto the gold particle. The conjugate IgG-AuNP was purified again by size exclusion (BioRad P100) and concentrated by ultracentrifugation. B. PAGE analysis of the starting IgG and of the conjugates before and after passivation with thiolated PEG. The left image shows the gel after Coomassie blue staining to detect the protein. The right images (left) shows the Coomassie blue stained gel that was further treated with silver for the amplification of gold particles. Data showed effective conjugation both by detection of gold and by the observation of a fully retarded band when PEG was attached onto the AuNP surface.

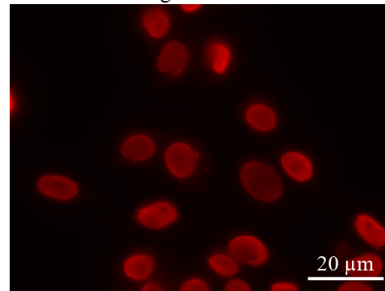
A. Immunodetection of the mouse anti-GFP antibody into the H2B-GFP HeLa



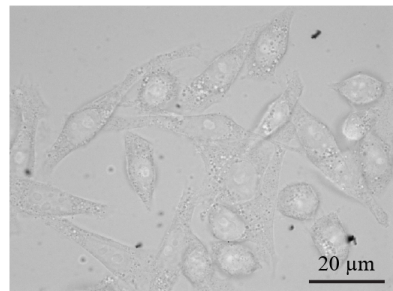
1. Detection of GFP



2. Detection of the secondary AlexaFluoro568 goat anti-mouse



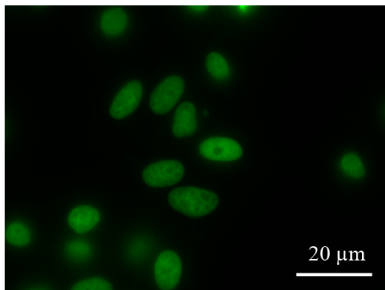
3. Silver enhancement IgG



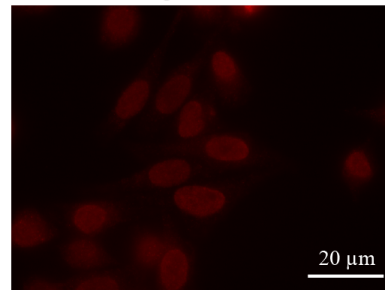
B. Immunodetection of the mouse anti-GFP antibody-AuNP conjugate



1. Detection of GFP



2. Detection of the secondary AlexaFluoro568 goat anti-mouse



3. Silver enhancement of the IgG bound AuNP

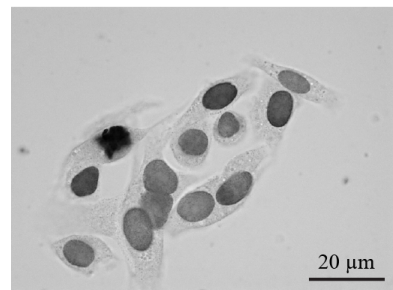


Figure S12. Fluorescent and silver-enhanced images of H2B-GFP HeLa cells after IgG and IgG-AuNP -mediated detection of GFP. The cells were fixed in 0.1M Sorenson buffer containing 4% PFA for 30 min and then permeabilization with 0.1% Triton X-100 in PBS. A. Immunodetection and silver enhancement of the mouse anti-GFP IgG (clone GFP-2A3) and of the corresponding AuNP conjugate were then performed using a secondary AlexaFluoro568 goat anti-mouse. B. Immunodetection and silver enhancement of the mouse anti-GFP IgG-AuNP conjugate. The permeabilized cells were incubated with 7 nM antibody or antibody conjugate in PBS containing 10% FBS.

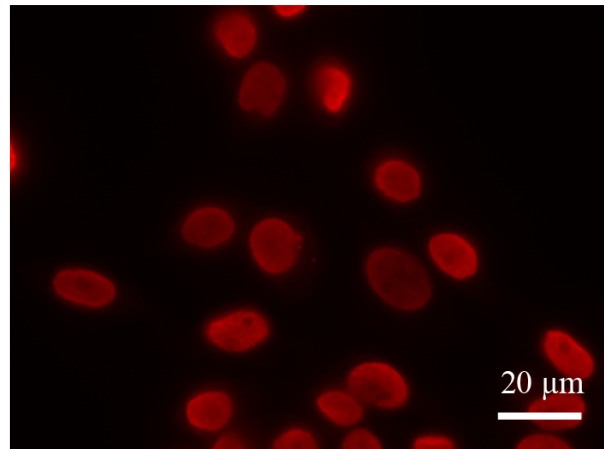
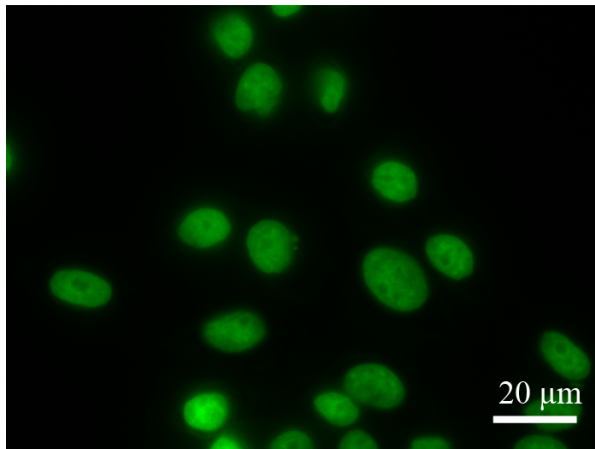
Immunodetection of the anti-GFP mouse antibody into H2B-GFP HeLa cells

Detection of the GFP

Detection of the mouse anti-GFP

with a AlexaFluoro568 goat anti-mouse

Fixation: 4% PFA



Fixation: 2% PFA, 0.02 % glutaraldehyde

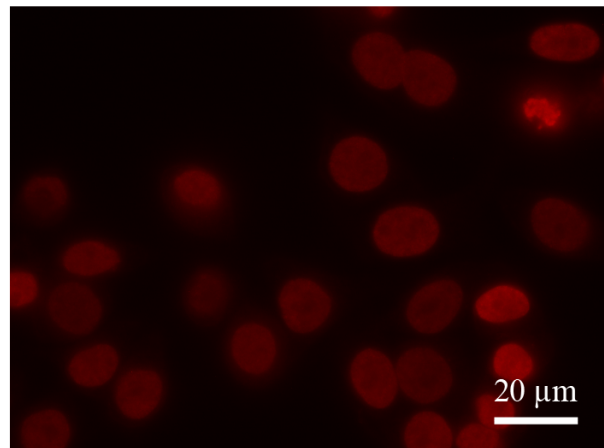
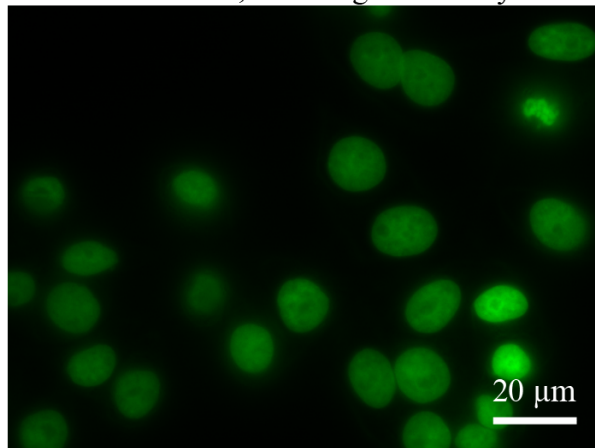


Figure S13. Fluorescent images of H2B-GFP HeLa cells after IgG-mediated detection of GFP. The cells were fixed in 0.2M HEPES buffer pH7.4 containing 4 % PFA or 2% PFA and 0.02% glutaraldehyde for 30 min. After permeabilization with 0.1% Triton X-100 in PBS (20 min), the GFP was bound by the mouse anti-GFP IgG (clone GFP-2A3, 7 nM in 10% FBS in PBS). After a washing step, the mouse anti GFP was detected with a secondary AlexaFluoro568 goat anti-mouse (7 nM).

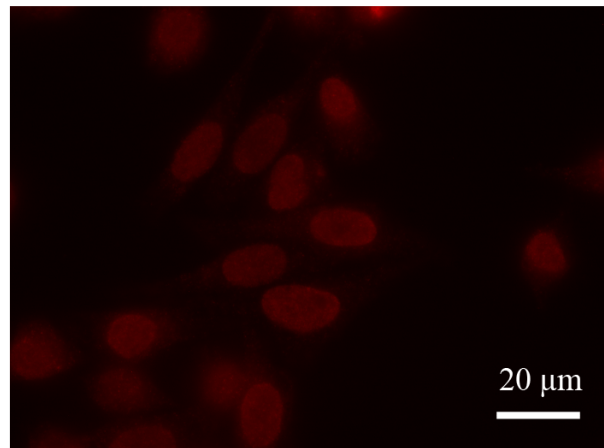
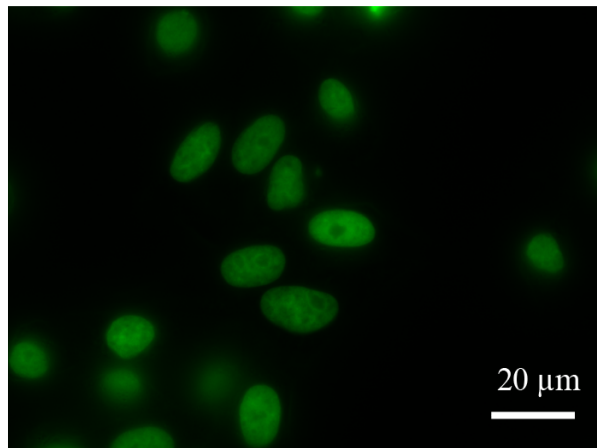
Immunodetection of the anti-GFP mouse antibody-AuNP conjugate into H2B-GFP HeLa

Detection of the GFP

Detection of the mouse anti-GFP

with a AlexaFluoro568 goat anti-mouse

Fixation: 4% PFA



Fixation: 2% PFA, 0.02 % glutaraldehyde

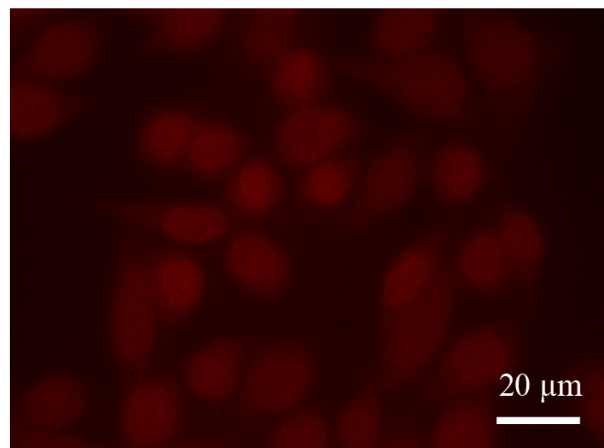
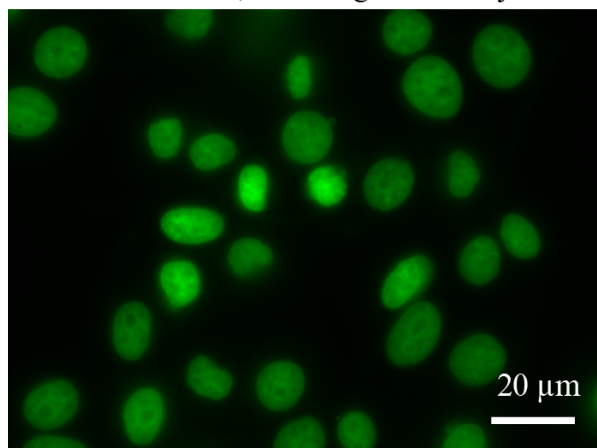
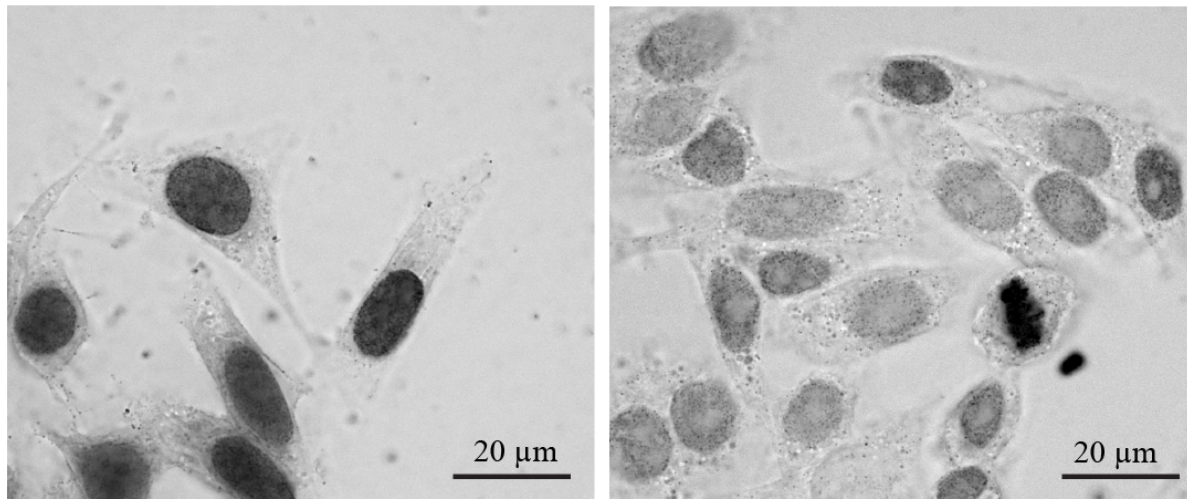


Figure S14. Fluorescent images of H2B-GFP HeLa cells after IgG-mediated detection of GFP. The cells were fixed in 0.2M HEPES buffer pH7.4 containing 4 % PFA or 2% PFA and 0.02% glutaraldehyde for 30 min. After permeabilization with 0.1% Triton X-100 in PBS (20 min), the GFP was bound by the mouse anti-GFP IgG-AuNP conjugate (7 nM in 10% FBS in PBS). After a washing step, the mouse anti GFP domain was detected with a secondary AlexaFluoro568 goat anti-mouse (7 nM).

1. $(\text{Nb-E})_2:(\text{K3})_2 \text{AuNP}$, 4 days storage at 4°C 2. $(\text{Nb-E})_2:(\text{K3})_2 \text{AuNP}$, 7 days storage at 4°C^*



3. $(\text{Nb-E})_2$, washing steps, then $(\text{K3})_2 \text{AuNP}$

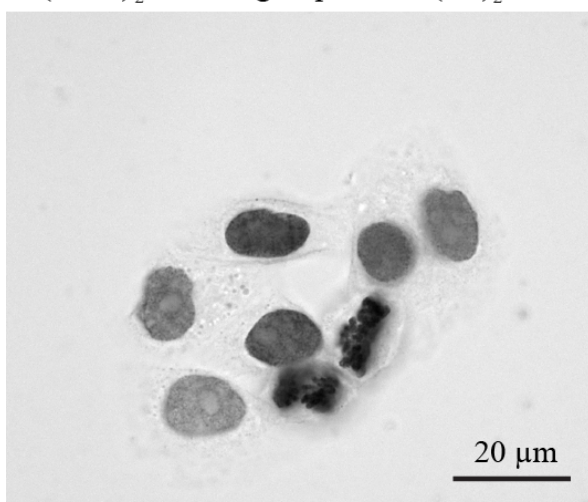


Figure S15. Analysis of $(\text{Nb-E3})_2:(\text{K3})_2 \text{AuNP}$ ability to detect GFP into H2B-GFP HeLa cells several days after assembly and evaluation of the sequential immunogold labelling methodology. Images 1 and 2. The $(\text{Nb-E3})_2:(\text{K3})_2 \text{AuNP}$ was assembled by mixing the $(\text{Nb-E3})_2$ with $(\text{K3})_2 \text{AuNP}$ in PBS (final concentration $2 \mu\text{M}$). The assembly was then stored at 4°C for 4 and 7 days before being used as immunogold labelling marker at a 10 nM concentration. Image 3. The fixed and permeabilized H2B-GFP HeLa cells were incubated first with 10 nM $(\text{Nb-E3})_2$ in PBS containing 10% FBS and then with 10 mM $(\text{K3})_2 \text{AuNP}$. Before incubation with the labelling markers, the cells were fixed with 0.2 M HEPES pH 7.4 containing 4% PFA (30 min) and the cell membrane were permeabilized with 0.1% Triton X-100.

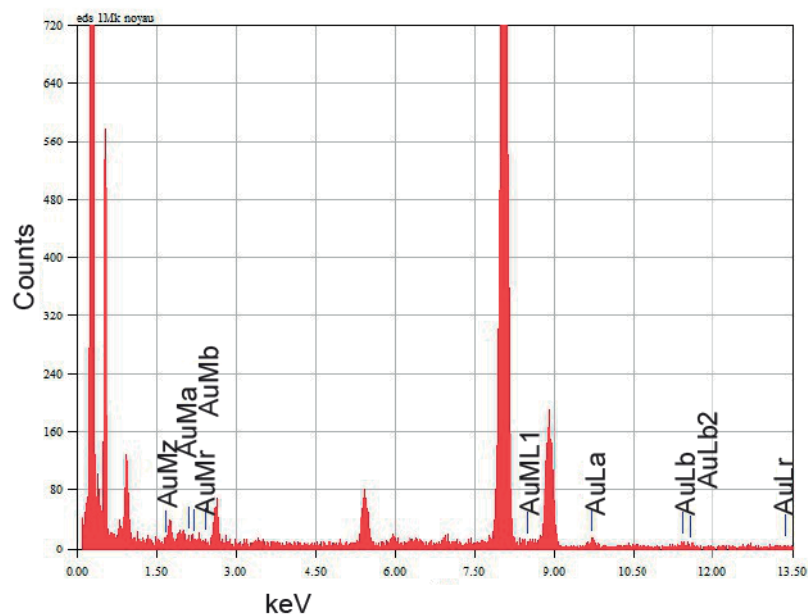


Figure S16. EDX spectroscopy analysis of a nuclear portion of H2B-GFP HeLa after gold immunolabeling with $(\text{Nb-E3})_2:(\text{K3})_2\text{AuNP}$ without silver-enhancement. The specimen was resin-embedded with the omission of the silver enhancement of the AuNP. The spectrum shows that the imaged nuclear area contains gold atoms. The intense peak at 0.277 keV is attributed to carbon and the intense peaks at 0.93 keV, 8.04 keV and 8.9 keV are attributed to copper, both resulting from the EM grids.

EDX spectroscopy analysis of a nuclear portion of H2B-GFP HeLa after gold immunolabeling with $(\text{Nb-E3})_2:(\text{K3})_2\text{AuNP}$ and silver-enhancement

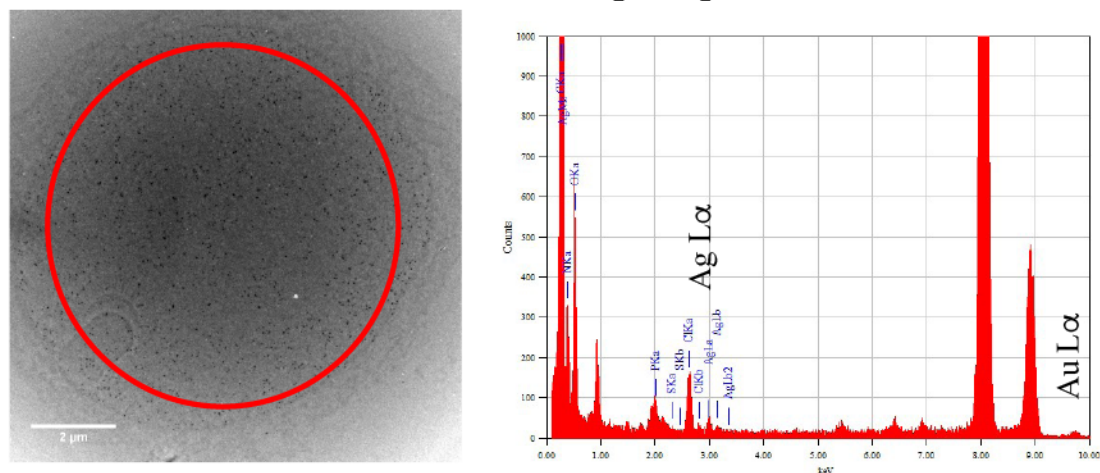
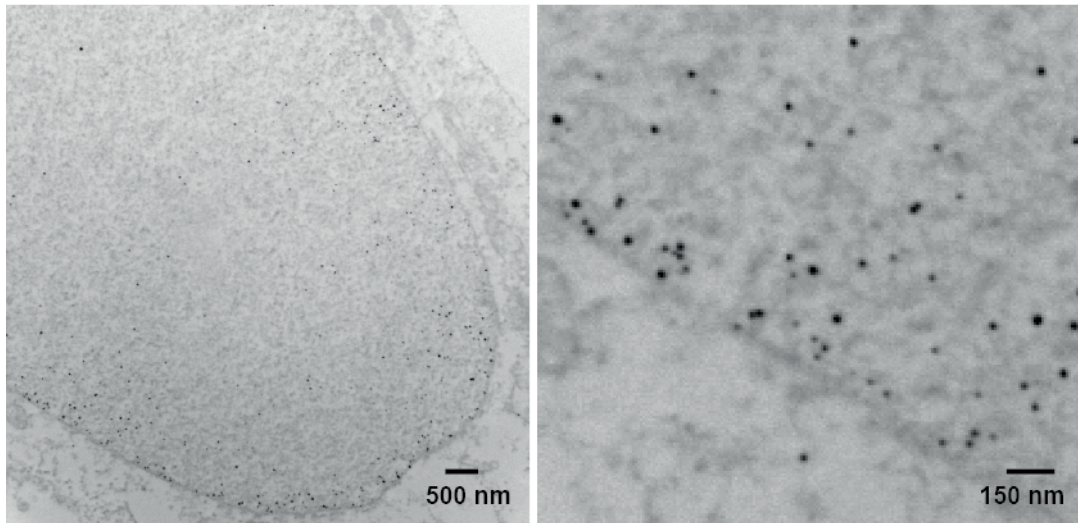


Figure S17. EDX spectroscopy analysis of nuclear portion of the H2B-GFP HeLa specimen after gold immunolabeling with $(\text{Nb-E3})_2:(\text{K3})_2\text{AuNPs}$ and silver enhancement. The spectrum indicate the presence of Au $L\alpha$ (9,712 eV) and Ag $L\alpha$ (2.984) signals suggesting that the silver deposition occurs on AuNP as claimed by Aurion, the manufacturer of the silver enhancement solution.

A. EM observation of $(\text{Nb-E3})_2:(\text{K3})_2\text{AuNP}$ labeled H2BGFP-HeLa



B. EM observation of $(\text{Nb-E3})_2:(\text{K3})_2\text{AuNP}$ labeled wild type HeLa

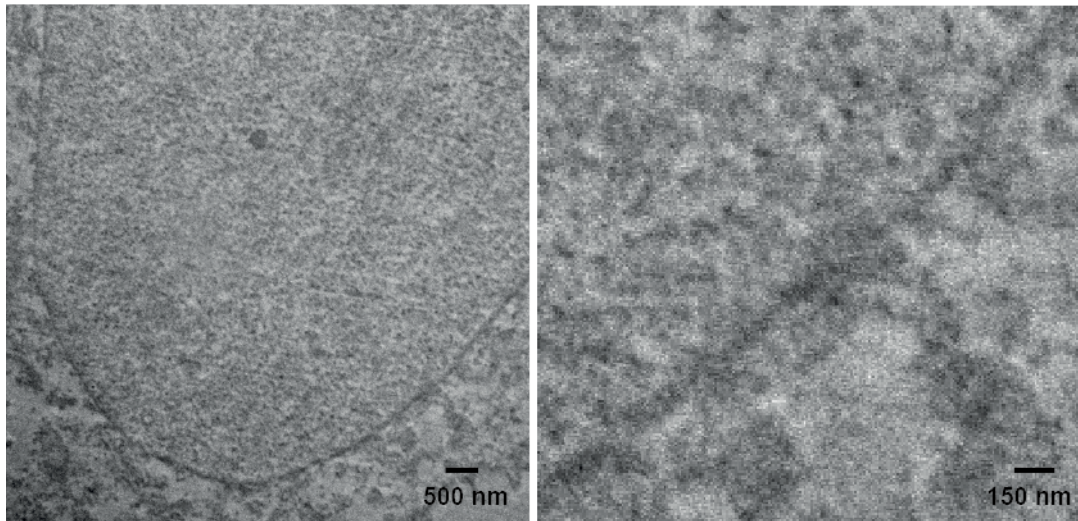


Figure S18. Pre-embedding immuno-EM of the histone protein H2B-GFP with $(\text{Nb-E3})_2:(\text{K3})_2\text{AuNP}$. After immunolabeling and post-fixation, AuNPs were silver enhanced and membranes stained with OsO_4 . Labels were seen only in the nuclei of H2B-GFP HeLa cells and not in the nuclei of the wild type HeLa.

References

- 1 N. Groybeck, A. Stoessel, M. Donzeau, E. C. da Silva, M. Lehmann, J.-M. Strub, S. Cianferani, K. Dembélé and G. Zuber, *Nanotechnology*, 2019, **30**, 184005.
- 2 X. Liu, M. Atwater, J. Wang and Q. Huo, *Colloids and Surfaces B: Biointerfaces*, 2007, **58**, 3–7.
- 3 D. Desplancq, N. Groybeck, M. Chiper, E. Weiss, B. Frisch, J.-M. Strub, S. Cianferani, S. Zafeiratos, E. Moeglin, X. Holy, A. L. Favier, S. De Carlo, P. Schultz, D. Spehner and G. Zuber, *ACS Applied Nano Materials*, 2018, **1**, 4236–4246.
- 4 M. H. Kubala, O. Kovtun, K. Alexandrov and B. M. Collins, *Protein Science*, 2010, **19**, 2389–2401.
- 5 G. Freund, D. Desplancq, A. Stoessel, R. Weinsanto, A.-P. Sibling, G. Robin, P. Martineau, P. Didier, J. Wagner and E. Weiss, *J. Mol. Recognit.*, 2014, **27**, 549–558.
- 6 B. M. Humbel, M. D. de Jong, W. H. Müller and A. J. Verkleij, *Microsc. Res. Tech.*, 1998, **42**, 43–58.
- 7 C. Chandrashekar, B. Pons, C. D. Muller, N. Tounsi, R. Mulherkar and G. Zuber, *Acta Biomater*, 2013, **9**, 4985–4993.